

## 3

6 <sup>1</sup>Indian Institute of Tropical Meteorology, Centre for climate change research, Ministry of  
7 Earth Sciences, India

8 <sup>2</sup>Leibniz-Institut für Troposphärenforschung, Leipzig, Germany,

<sup>3</sup>Department of Civil, Environmental and Geomatic Engineering, University College London,  
London, United Kingdom

11 <sup>4</sup>School of Earth and Environment, University of Leeds, Leeds, UK.

12 <sup>5</sup>Forschungszentrum Jülich GmbH, IEK-7, Jülich, Germany

13 Corresponding author email: suvarna@tropmet.res.in

The rapid melting of glaciers in the Hindu Kush Himalayas (HKH) during recent decades poses an alarming threat to water security for larger parts of Asia. If this melting persists, the entire Himalayan glaciers is estimated to disappear by end of 21st century. Here, we assess the influence of the spring 2020 COVID-19 lockdown on the HKH, demonstrating the potential benefits of a strict emission reduction roadmap. Chemistry-climate model simulations, supported by satellite and ground measurements, show that lower air pollution during lockdown led to a reduction in black carbon in snow (2-14%) and thus in snow melting (10-40%). This caused increases in snow cover (6-12%) and mass (2-20%) and a decrease in runoff (5-55%) over the HKH and Tibetan Plateau, ultimately leading to an enhanced snow-water-equivalent (3.3–55%). We emphasize the necessity for immediate anthropogenic pollution reductions to address the hydro-climatic threat to billions of people in South Asia.



## 1. Introduction

The Hindu Kush Himalayan (HKH) mountains and Tibetan plateau is the largest snow-cladded region outside the Poles (Fig. 1). The HKH meltwater feeds rivers in India and China that drive the agriculture, hydropower generation, and economy of these countries (Hussain et al., 2019, Sabin et al., 2020, Lee et al., 2021a). The Himalayan snowmelt in spring provides ~50% of the annual freshwater to ~4 billion people of South Asia and East Asia (sabin et al., 2020, Sarangi, et al., 2019). ~~Although snowmelt benefits freshwater supply to people, rapid Himalayan snowmelt caused a loss of ~40 % of the Himalayan glacier area compared to the Little Ice Age, 400 to 700 years ago, i.e. ~0.92 to 1.38 mm sea-level equivalent (Lee et al., 2021b). The snow mass over the Himalayas has generally decreased during the last 30 years (except for a few Karakoram glaciers that show an increasing trend in snow mass). The alarming rate of snow melting of 0.02 to 0.6 cm °C<sup>-1</sup> day<sup>-1</sup> raised concerns about the sustainability of water supply and loss of glaciers in the region (Hussain et al., 2019, Lee et al., 2021b, Tiwari et al., 2015). Model simulations for extreme scenarios show that Himalaya snow melting could cause the glaciers to disappear by the end of the 21<sup>st</sup> century (Cruz et al., 2007, Hock et al., 2019).~~

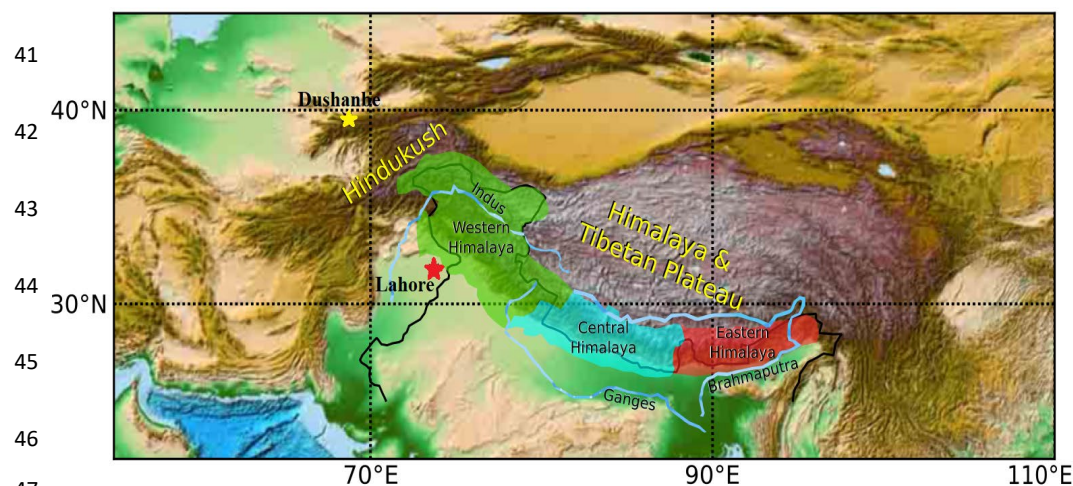


**Figure 1:** Map of the Hindu Kush Himalayas region with the Western (70 - 80° E, 30° - 35° N), Central (80° - 87° E, 28° - 30° N), and Eastern Himalayas (88° - 95° E, 26° - 30° N). A yellow



50 and red star indicates the location of the AERONET sun photometer stations Dushanbe  
51 (68.858° E, 38.553 ° N) and Lahore (74.264° E, 31.480° N), respectively.

52       The accelerated thinning of Himalayan glaciers is attributed to climate change causing  
53 shifts in air temperature and precipitation, as well as the atmospheric distribution and  
54 deposition of light-absorbing particles i.e., dust, black carbon (BC) (IPCC 2013, Krishnan et  
55 al., 2019). Among the aforementioned factors, snow darkening due to the deposition of  
56 absorbing aerosols is an integral component of Himalayan snowmelt and runoff (Lau et al.,  
57 2010). The snow-melting efficacy of BC is higher than that of greenhouse gases (Sarangi et al.,  
58 2019, Qian, et al., 2011, Nair, et al., 2013, Ma et al., 2019). The increasing energy demand of  
59 the densely populated South Asian region has increased the emission of greenhouse gases and  
60 BC aerosol in the last few decades (Fadnavis et al., 2017, Krishnan et al., 2020), leading to  
61 enhanced darkening and snow melting (Usha et al., 2021).

62

63       The economic slowdown caused by the COVID-19 pandemic measures led to a drastic  
64 reduction in public and freight transportation, industrial emissions, and energy use (Fadnavis  
65 et al., 2021). This resulted in a substantial decline in emissions of several atmospheric  
66 pollutants including greenhouse gases and black carbon aerosol (Forster et al., 2020, Kanniah  
67 et al., 2020, Le Quéré et al., 2020) and potentially reduced deposition of dark aerosols on snow  
68 and ice (Bair et al., 2021). Remote sensing observations show cleaner snow with ~30% less  
69 light-absorbing impurities in snow during the lockdown period over Asia between March and  
70 May 2020 (Bair et al., 2021). This led to decreased snowmelt by 25 – 70 mm in 2020 compared  
71 to the last 20-year mean over Western Himalayas due to decreased radiative forcing induced  
72 by BC and dust deposition on snow/ice surfaces and related changes in ~~in~~ snow absorption and  
73 surface albedo (Bair et al., 2021). Impacts of reduced levels of air pollution on changes in the  
74 snow mass, surface water runoff, and water reservoir over the HKH are not reported hitherto.



Here, we provide a detailed analysis of the impact of reduced pollution over HKH and Tibetan plateau region during the COVID-19 lockdown period between March and May 2020. We used global simulations with the chemistry-climate model ECHAM6-HAMMOZ (Tegen et al., 20219, Schultz, et al., 2018) updated with an improved BC-in-snow parameterization, in order to contrast the COVID-19 (COVID) with the typical, unchanged (control, CTL) air pollution conditions. The COVID simulations are performed using a COVID-19 emission inventory where emissions are reduced based on Google and Apple mobility data (Forster, et al., 2020) (details in Appendix A).

## 2. Results

### 2.1 Reduction of airborne aerosols and in-snow BC concentration over the Himalayas

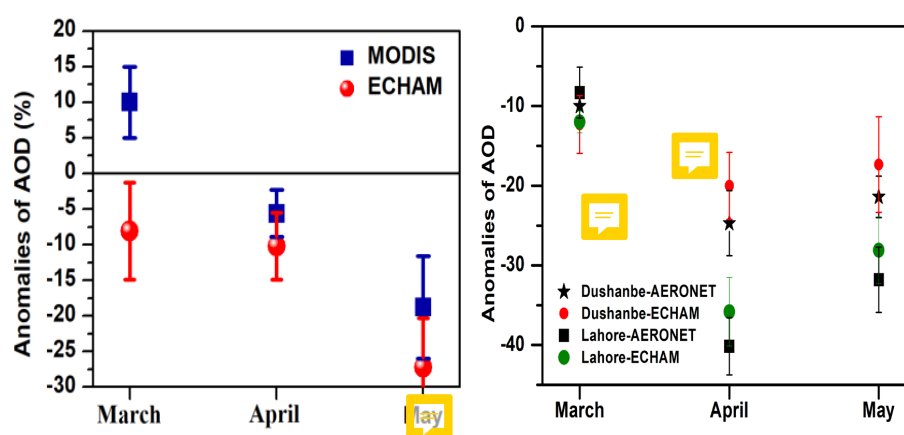


**Figure 2:** (a) Changes in monthly mean AOD (%) during March - May 2020 from MODIS in comparison to mean of 2001-2019 and ECHAM-HAMMOZ (COVID minus CTL) averaged over the Hindu Kush Himalayas (HKH) and Tibetan Plateau region (75° - 95° E, 30° - 35° N), (b) same as (a) but for AOD from AERONET observations and ECHAM-HAMMOZ model results at Dushanbe (68.858° E, 38.553° N, climatology 2010-2019) and Lahore (74.264° E, 31.524° N, climatology 2010-2019).



99 31.480° N, climatology 2006-2019). Vertical bars in Fig (a)-(b) indicate the standard deviation  
 100 within ten members of model simulations.




101

102 The COVID-19 lockdown restrictions in spring 2020 decreased the anthropogenic  
 103 aerosol amounts over the HKH ranges (Western, Central, and Eastern Himalayas), and the  
 104 Tibetan Plateau region. The ECHAM6-HAMMOZ model simulations show that COVID  
 105 lockdown resulted in a cleaner atmosphere during March - May 2020 over the HKH ranges and  
 106 Tibetan Plateau region. There is a reduced level of Aerosol Optical Depth (AOD) over the  
 107 region throughout spring 2020 by  $-8.1 \pm 6.2$  % in March,  $-10.2 \pm 4.7$  % in April,  $-27 \pm 6.9$  % in  
 108 May compared to the CTL (non COVID) simulation (Fig. 2a). This is supported by NASA's  
 109 Moderate Resolution Imaging Spectroradiometer (MODIS) measurements also showing a  
 110 reduction in AOD in April ( $-5.6 \pm 3.3$  %) and May ( $-18.8 \pm 7.2$  %) 2020 compared to the mean  
 111 over the last 20 years (Fig 2a). Thus, both model simulations and MODIS AOD show a  
 112 reduction in aerosol pollution in April - May 2020. For March 2020, MODIS measurements  
 113 show AOD enhancement by  $10.2 \pm 4.8$  %, which is due to increased dustiness over the HKH  
 114 region (see Appendix B for a detailed discussion). AOD measurements at two Aerosol Robotic  
 115 Network (AERONET) sun photometer stations in Dushanbe ( $68.858^\circ$  E,  $38.553^\circ$  N),  
 116 and Lahore ( $74.264^\circ$  E,  $31.480^\circ$  N) show an AOD reduction in agreement with our model  
 117 simulations (Fig. 2b). There are differences among MODIS, AERONET and the model. The  
 118 changes in AOD during COVID compared to no-COVID period is smaller in the model than  
 119 the MODIS observations by 4.2 - 9.8 % and larger than the AERONET observations by 1.8  
 120 - 4.2 %. These differences are due to the fact that the simulated AOD change is in response to  
 121 the reduction of anthropogenic aerosols and associated circulation responses, while MODIS  
 122 and AERONET measurements show the effect of all atmospheric processes. Also, note that the  
 123 MODIS AOD values are spatial averages representative for a relatively large area while the  
 124 AERONET values are point measurements. Importantly, changes in simulated AOD in 2020



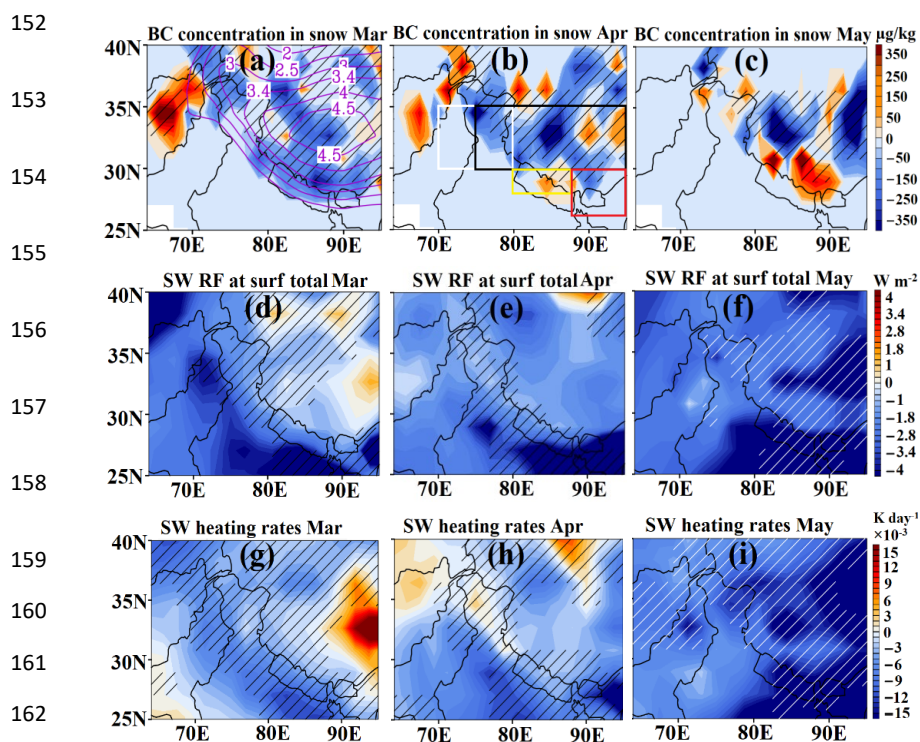
125 fall within the standard deviation of satellite and ground-based measurements indicating  
 126 reliability of our simulations (except for March 2020 with respect to MODIS). Our model  
 127 simulations also show a reduction in BC burden by 15 -55% (Fig. S1a), and sulfate burden by  
 128 22 - 24 % over the HKH and Tibetan Plateau regions in spring 2020 (Fig. S1b). Interestingly,  
 129 dust burden also shows a reduction over these regions (Fig. S1c and Fig. S2), except over  
 130 central Himalaya in March and April 2020 (details in Appendix B). A drop in BC is also  
 131 observed in Aerosol Radiative Forcing Over India Network (ARFINET) ground-based  
 132 measurements over the Indo-Gangetic Plain ( $> 50\%$ ), north-eastern India ( $>30\%$ ), Himalaya  
 133 regions (16 - 60%), and Tibet (70%) during spring 2020 (Gogoi et al., 2020, Liu et al., 2020)  
 134 Similar impact of reduction of energy consumptions on decrease in AOD during the COVID-  
 135 19 lockdown period, i.e., in spring 2020 compared to the 2010-2019 climatology are also seen  
 136 over South and East Asia (40 %) and Indo-Gangetic Plain (IGP) by 30 – 40 % in satellite  
 137 measurements (Fadnavis et al., 2021, Srivastava et al., 2021, Pandey et al., 2021, Shafeeqe et  
 138 al., 2021).

139

140 The reduction in anthropogenic air pollution leads to a reduction in BC concentration  
 141 in the snow  $\sim 25 - 350 \mu\text{g kg}^{-1}$  (by  - 35 %) during spring 2020 (Fig. 3a-c) that reduce the  
 142 snow darkening effect by embedded aerosol impurities. Our simulations reveal that the  
 143 decrease in BC concentration in the snow has decreased the shortwave radiative forcing at the  
 144 surface by  $0.2 - 2 \text{ W m}^{-2}$  in March - May 2020 (Fig. 3 d-f), leading to a decrease in tropospheric  
 145 heating by solar radiation of 0.001 to  $0.015 \text{ K day}^{-1}$  (Fig. 3 g-i). The reduced BC in the  
 146 atmosphere over the HKH and Tibetan Plateau region resulted in less absorption and re-  
 147 emission of longwave radiation and, as a consequence, there is a reduction in longwave  
 148 radiative forcing in the atmosphere leading to a lower atmospheric heating (Fig. S3). Therefore,  
 149 the reduction of anthropogenic sulfate, and BC burden, combined with lower atmospheric



150 loadings of BC, PM2.5 and PM10, as well as BC in snow resulted in decreased heating of the  
 151 snowpack and tropospheric column.



164 **Figure 3:** Spatial distribution of anomalies (COVID minus CTL) of BC concentration in snow  
 165 ( $\mu\text{g kg}^{-1}$ ) for (a) March, (b) April, and (c) May 2020; (d-f) shortwave radiative forcing ( $\text{W m}^{-2}$ )  
 166 at the surface and (g-i) tropospheric heating rates ( $\text{K day}^{-1}$ ) due to changes in BC  
 167 concentration in snow (COVID minus CTL). Hatched areas indicate the 95%-significance  
 168 level. Contours in panel (a) indicate topography in km. Boxes in panel (b) indicate boundaries  
 169 of Western Himalayas (WH, white), Central Himalayas (CH, yellow), Eastern Himalayas (EH,  
 170 red) and Tibetan Plateau (black).

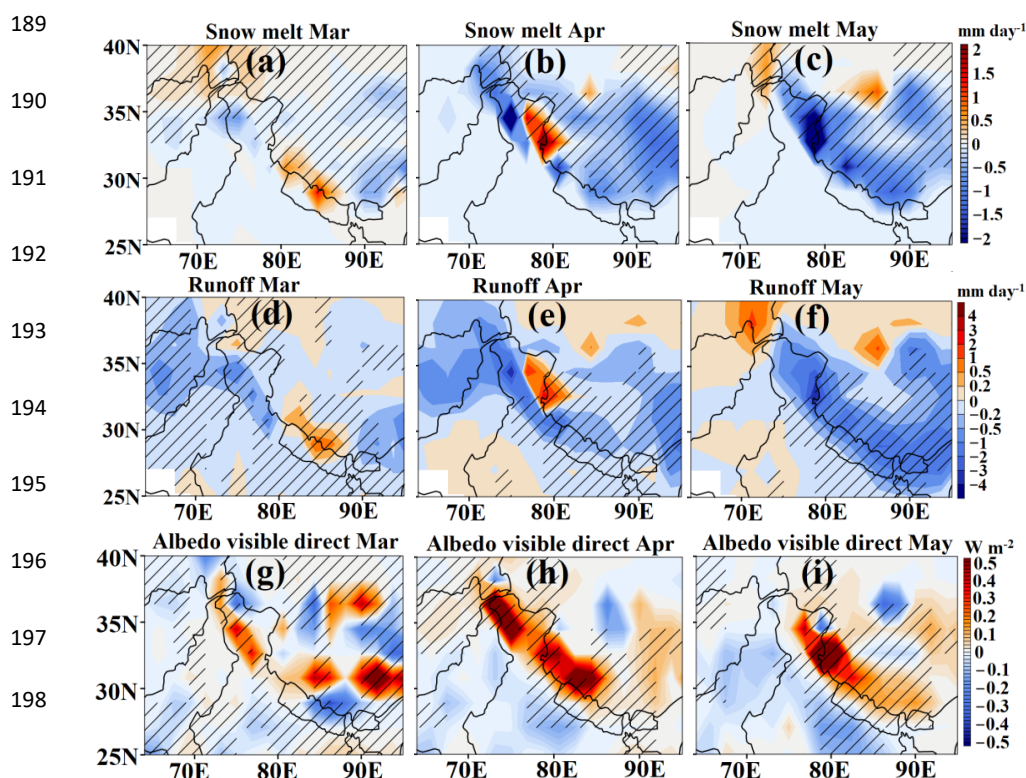
## 172 2.2 Impacts on snow melting, surface water runoff, and snow cover

173 Further we show that the decrease in aerosol pollution reduced the snow melting in  
 174 spring 2020 by 0.2 to 2.5  $\text{mm day}^{-1}$  corresponding to 10 – 50 % (Fig. 4 a-c). The amount of  
 175 reduction of snow melting is pronounced over the western Himalayas in May. As a result of a





176 reduction in snowmelt, surface water runoff has been drastically reduced by 2-4 mm day<sup>-1</sup> (5 -  
 177 55 %) (Fig. 4 d-f). The reduction in the runoff is most pronounced in May over the entire  
 178 Himalayas and central Tibetan Plateau region. Estimates from remote sensing measurements  
 179 also show the reduction of runoff by 6.5 km<sup>3</sup> of melted water in the Indus River Basin (Bair et  
 180 al., 2021). In the past, studies have shown that elevated levels of light-absorbing aerosols  
 181 (elemental carbon: 13 to 75 ng g<sup>-1</sup> and dust: 32 to 217 µg g<sup>-1</sup>) can contribute to about 3 to  
 182 10 mm day<sup>-1</sup> of snowmelt over western Himalayas (Thind et al., 2019). Sensitivity analysis  
 183 using a glacier mass balance model shows that a BC-induced snow albedo reduction resulted  
 184 in an increase in runoff by 4 – 18% annually (Santra, et al., 2019). In contrast to impacts of  
 185 rising anthropogenic emissions during the past decades, emission reductions during the 2020  
 186 COVID-19 lockdown period caused a brighter albedo that led to an enhanced reflection of 0.2  
 187 - 0.5 W.m<sup>-2</sup> (see Fig. 4g-i), reducing atmospheric heating, snow melting and runoff in spring  
 188 2020.

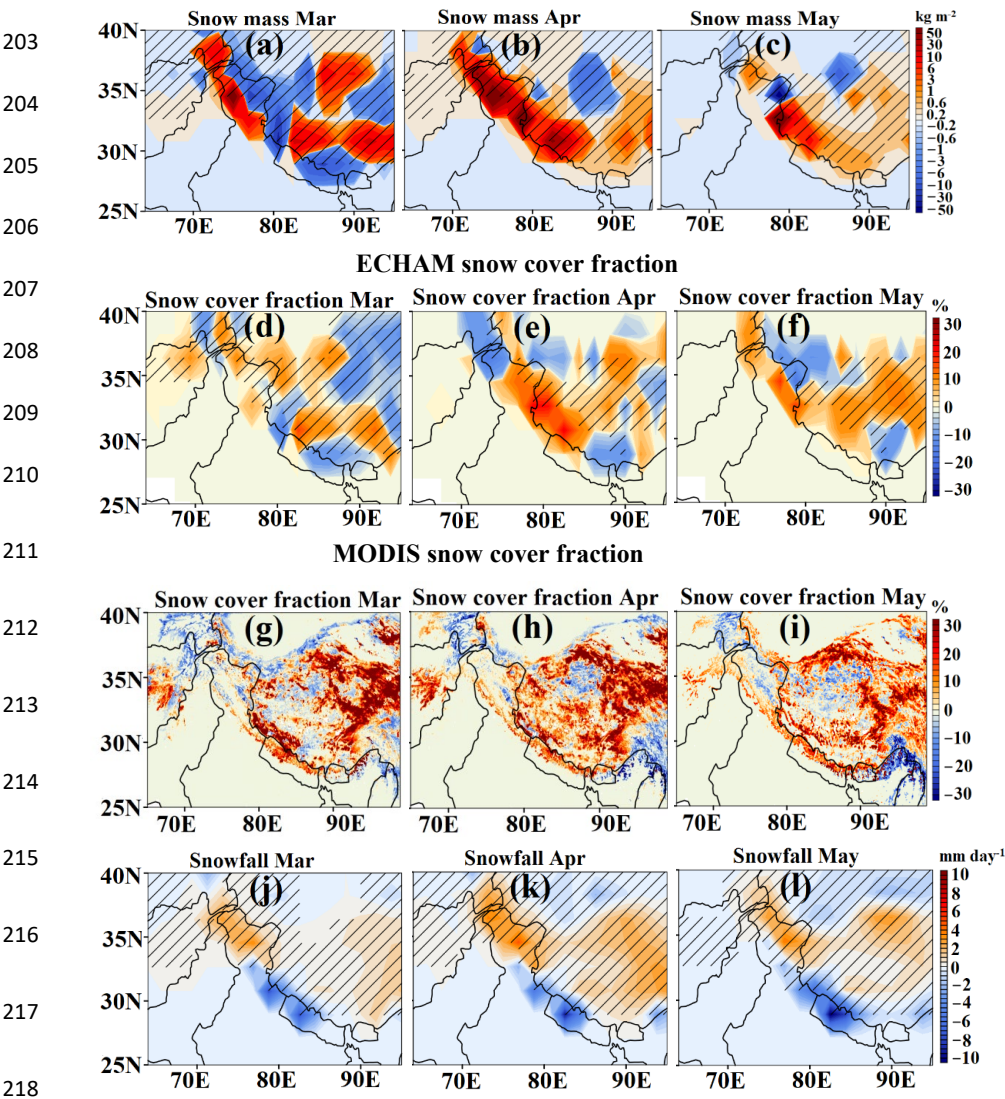






199 **Figure 4:** Spatial distribution of anomalies of (a-c) snow melt ( $\text{mm day}^{-1}$ ), (d-f) surface water  
200 runoff ( $\text{mm day}^{-1}$ ) for March to May 2020 (COVID minus CTL) and (g-i) surface albedo mean  
201 in the visible ( $\text{W m}^{-2}$ ). Hatched areas indicate the 95%-significance level.

202



219 **Figure 5:** Monthly mean anomalies (COVID minus CTL) of the (a-c) snow mass ( $\text{kg m}^{-2}$ ), and  
220 (d-f) snow cover fraction (%) for March to May 2020 as modelled by ECHAM6-HAMMOZ  
221 as well as (g-i) snow cover fraction anomalies from MODIS satellite measurements (%) with  
222 respect to the climatological average 2000-2019. (j-l) monthly mean anomalies of the snowfall





223 for March to May 2020 as modelled by ECHAM6-HAMMOZ (COVID minus CTL). Hatched  
 224 areas indicate the 95%-significance level.

225

226 Our simulations also indicate that these changes lead to an increase in snow mass of  
 227 0.2-50 kg m<sup>-2</sup>, i.e. 10-40% (Fig. 5a-c) and snow cover fraction of 2-30% during spring 2020  
 228 (Fig. 5d-f). MODIS measurements (Fig. 5g-i) also show a remarkable agreement with the  
 229 model simulations (especially during April - May 2020), with increased snow cover of about  
 230 15-30% over the parts of Western Himalayas and Central Himalayas and the Tibetan Plateau  
 231 region and decreased by 5-12 % over parts of North-East Himalayas especially in April and  
 232 May 2020. However, there are also some differences in terms of exact regions of snow cover  
 233 enhancement or reduction respectively, since the MODIS observations include the influence of  
 234 real-time meteorology, while meteorology in the model ensemble include internal variability.  
 235 Our model simulations show that pollution changes in COVID-19 lockdown period and  
 236 associated changes in meteorology has increased snowfall (2-5 mm day<sup>-1</sup>, 3-20 %) over the  
 237 Western Himalayas and Tibetan Plateau region (Fig 5j-i). The increase in snowfall over these  
 238 regions will contribute to enhancement in snow mass and snow cover (Fig. 5 a-i) and albedo  
 239 (Fig. 4 g-i).

240

241 The impact of reduced pollution on the snow water in the Himalayas from our model  
 242 simulations is illustrated in Fig. 6a. The snow mass enhancement led to increase in the snow  
 243 water equivalent by 2.1 to 14.7 mm (3.3 to 55 %). The Western Himalayas show the highest  
 244 increase in snow water equivalent by 14.7 mm (55 %) followed by the Tibetan Plateau by 12  
 245 mm (by 22 %) and Central Himalayas by 10 mm (by 18%) in April. While the Eastern  
 246 Himalayas show a decrease in March (-1.3 mm; 10 %) and small enhancement in April by  
 247 2.1mm (3.3 %) and May 2020 by 2.3 mm (3.7%) due to pollution reduction. Thus, human  
 248 induced pollution reduction during the COVID-19 lockdown benefitted the HKH in many



ways. A schematic shows the COVID-19 lockdown-induced effects in Figs. 6b-c: increased snow surface reflectivity, reduced snowmelt and surface water runoff, as well as enhanced snow water.

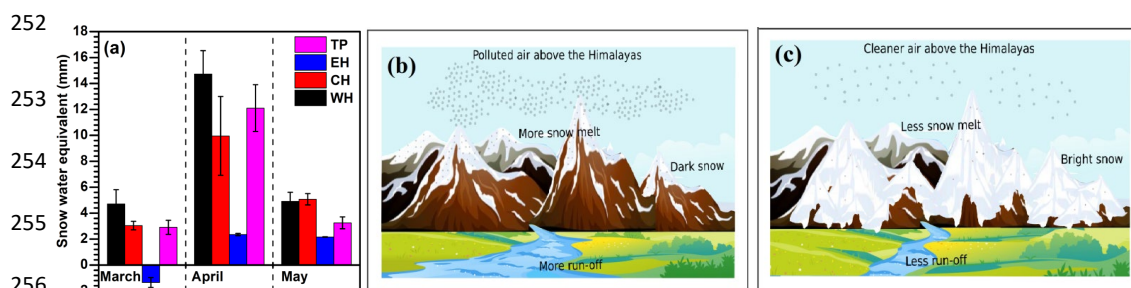


**Figure 6:** (a) Anomalies (CTL minus COVID) in snow water equivalent (mm) from March to May 2020 over the Western Himalayas (WH), Central Himalayas (CH), Eastern Himalayas (EH) and Tibetan Plateau (TP). Vertical bars indicate the standard deviation within ten members of model simulations. Schematic illustrating the impacts of (b) air pollution on snow darkening in the Himalayas and surface water runoff than for usual polluted case and (c) the impacts of reduced pollution on snow brightening in the Himalayas and reduced surface water runoff, as observed during the 2020 COVID-19 lockdown period.

264

**3. Summary and conclusions:** A rising trend in Asian air pollution and associated climate change over the last few decades have had a detrimental impact on snow melting over the Hindu Kush Himalayas (HKH) and Tibetan Plateau region<sup>32</sup>. Black carbon from increasing emissions of biomass burning, industrial and domestic combustion and transport is deposited on snow, reducing its albedo (i.e. darkening). A snow darkening effect, compounded with other climate change effects, accelerates the melting of snow and the disappearance of ice cover over the HKH and Tibetan Plateau region at an extraordinary rate (Usha et al., 2021). The drop in anthropogenic air pollution emissions, e.g. from energy production, during the COVID-19 lockdown period in spring 2020 reduced air pollutant levels worldwide (Forster, et al., 2020). Our model simulations indicate that the associated reduction in anthropogenic aerosols and greenhouse gases in spring 2020 have benefited the HKH. It



276 caused an enhancement in the snow cover fraction by 6 - 12 % and snow mass by 2 - 20 %,  
 277 corresponding to a decrease in snow melting by 10 – 40 % and surface water runoff by 0.2 - 3  
 278 mm day<sup>-1</sup>. As a consequence, the amount of snow water equivalent is increased considerably  
 279 by 3.3 to 55 %.

280 Our findings highlight that out of the two processes causing a retreat of Himalayan  
 281 glaciers: (1) a slow response to global climate change and (2) a fast response to local air  
 282 pollution (especially black carbon), a policy action on the latter is more likely to be within  
 283 reach of possible policy action on a shorter-term time scale. Even if we stopped CO<sub>2</sub> emissions  
 284 immediately, temperatures would not start decreasing. Our findings confirm the importance of  
 285 reducing short-lived climate forcers (Black carbon) and their complementary role to CO<sub>2</sub>  
 286 mitigation (Rogelj et al., 2014). Reduction of air pollution to levels similar with those recorded  
 287 during the 2020 COVID-19 lockdown period, could safeguard HKH glaciers, which are  
 288 otherwise under the threat to disappear by 21<sup>st</sup> century. Since 2000 Himalayan glaciers have  
 289 been losing nearly half a meter of ice a year (Wester et al., 2019). Our estimates indicate that  
 290 air pollution reduction during COVID 19 lockdown in spring 2020 caused reduction in snow  
 291 melt by 0.5 to 1.5 mm day<sup>-1</sup>, indicating large benefits to HKH glaciers. Even if global warming  
 292 is kept below 1.5°C, one third of the glaciers in the HKH region and more than half of those in  
 293 the Eastern Himalaya will likely be lost by the end of this century (Bolch et al., 2019). The  
 294 speedily retreating glaciers and the snowpack loss are already posing a threat to domestic  
 295 sustainable water resources for billions of people in Asia (Wood et al., 2020). However, if new  
 296 economically and technically feasible policies would reduce emissions of air pollutants (in  
 297 particular black carbon) to at least lockdown period levels, snowmelt could be reduced by 10  
 298 – 50%. Such policies will therefore bring substantial benefits for sustained water supply,  
 299 agriculture, and ecosystems in large parts of Asia.



## 300 **Appendix A: Methods:**

### 301 **A1.1 Observational data**

302 We used monthly snow cover fraction from NASA's Moderate Resolution Imaging  
 303 Spectroradiometer (MODIS) satellite product on a 0.5x0.5° resolution (version 6, level 3) (Hall  
 304 et al., 2006) for the years 2000 – 2020 (<https://nsidc.org/data/MOD10CM/versions/6>). For  
 305 aerosol information we used monthly mean satellite AOD at 1x1° resolution from the MODIS  
 306 Terra level-3 dark target and deep blue retrievals at 550 nm wavelength for 2001-2020  
 307 (<https://giovanni.gsfc.nasa.gov>). We also used ground-based sun photometer observations of  
 308 AOD from the Aerosol Robotic Network (AERONET) (Martonchik et al., 2004) at the stations  
 309 Dushanbe (68.858° E, 38.553° N) for the period 2010-2020 and Lahore (74.264° E, 31.480° N)  
 310 for the period 2006 – 2020, situated in HKH region (<https://aeronet.gsfc.nasa.gov>).

311

### 312 **A1.2 The ECHAM6-HAMMOZ model description and Experimental set-up**

313 We performed 10-member ensemble experiments using the state-of-the-art aerosol-  
 314 chemistry-climate model ECHAM6-HAMMOZ (version echam6.3-ham2.3-moz1.0 (Schultz,  
 315 et al., 2018, Tegan et al., 2019). The model comprises the atmospheric general circulation  
 316 model ECHAM6 (Stevens et al., 2013), the tropospheric chemistry module (Schultz, et al.,  
 317 2018), and the Hamburg Aerosol Model (HAM) (Stier et al., 2005, Zhang et al., 2012). The  
 318 HAM component predicts the nucleation, growth, evolution, and sinks of sulphate ( $\text{SO}_4^{2-}$ ),  
 319 black carbon (BC), organic carbon (OC), sea salt (SS), and mineral dust (DU) aerosols. Seven  
 320 log-normal modes describe the size distribution of the aerosol population with a prescribed  
 321 variance in the aerosol module. The MOZ submodule describes the trace gas chemistry from  
 322 the troposphere to the lower thermosphere. The chemical mechanism includes the  $\text{O}_x$ ,  $\text{NO}_x$ ,  
 323  $\text{HO}_x$ ,  $\text{ClO}_x$  and  $\text{BrO}_x$  chemical families, along with  $\text{CH}_4$  and its degradation products. Several



324 primary non-methane hydrocarbons (NMHCs) and related oxygenated organic compounds are  
 325 also described. It contains 108 species, 71 photolytic processes, 218 gas-phase reactions and  
 326 18 heterogeneous reactions with aerosol (Schultz, et al., 2018). Details of emissions  
 327 (anthropogenic, biomass burning, biogenic, fossil fuel etc.) and model parametrisation and  
 328 other details are reported in the past (Fadnavis, et al., 2017, 2019,a,b 2021). Anthropogenic and  
 329 biomass burning emissions of sulphate, and black carbon (BC) and organic carbon (OC) are  
 330 based on the AEROCOM-ACCMIP-II emission inventory for year 2020 (Lamarque et al.,  
 331 2010, Textor et al., 2006). Additional consideration for the reduction of snow albedo due to  
 332 BC in snow is implemented but extended for the MOZ module (Huang, 2018). Snow albedo  
 333 reduction is calculated by considering the concentration of BC in the top layer of surface snow.  
 334 Influxes of BC in snow include below-cloud and in-cloud wet scavenging, as well as dry  
 335 deposition and sedimentation. Snowmelt and glacier runoff remove the in-snow BC at a  
 336 reduced efficiency, leading to enhanced concentration, while fresh and pristine snowfall leads  
 337 to reductions in BC concentration.

338

339 The model simulations were performed at T63 horizontal resolution ( $1.875^\circ \times 1.875^\circ$ ) with 47  
 340 levels in the vertical from the surface to 0.01 hPa (corresponding to approx. 80 km), and with  
 341 a time step of 20 minutes. To understand the effect of the COVID-19 restrictions on snow over  
 342 Himalayas and Tibetan plateau region we conducted a control (CTL) and a COVID-19  
 343 (COVID) simulation. We adopted an ensemble approach (with 10 ensemble members) for the  
 344 above two experiments. Ten spin-up simulations were performed from 1 to 31 December 2019  
 345 to generate stabilised initial fields for the 10 ensemble members. Emissions were the same in  
 346 each of the 10 members during the spin-up period. Control simulations were extended with the  
 347 same setup until 1 July 2020. While for the COVID simulations (10 ensemble members each),  
 348 the anthropogenic emission of all gases and aerosols were changed since 1 January 2020





349 according to Google and Apple mobility data (Forster et al., 2020). The COVID-19 emissions  
 350 were prepared by deriving scaling factors between the input4MIPS SSP245 baseline and the  
 351 version5, 2-year blip scenario (Forster et al., 2010), separately for each species and each grid  
 352 point (see Fig. S4a). Subsequently, these scaling factors have been applied to the AeroCom-II  
 353 ACCMIP emissions. This ensures consistency of the drop in emissions independent of the  
 354 absolute emission values in the AeroCom-II ACCMIP and the input4MIPS SSP245 data sets.  
 355 The global mean emission changes in carbon monoxide (CO, 2-24%), black carbon (BC, 3-  
 356 23%), organic carbon (OC, 2-17%), sulfur dioxide (SO<sub>2</sub>, 3-23%), nitrogen oxides (NO<sub>x</sub>, 2-  
 357 30%), methane (CH<sub>4</sub>, 2-5%), and ammonia (NH<sub>3</sub>, 0-3%) during the period January to 1 July  
 358 2020 (COVID - CTL) are in agreement with previous studies (Foster et al., 2020, Le Quéré et  
 359 al., 2020) (Fig. S4b). The COVID and CTL simulations ended on 1 July 2020. To investigate  
 360 the effects of COVID-19 emissions in spring (i.e., since 1 March 2020), we analysed the  
 361 difference between COVID and CTL simulations for the spring season in 2020. The same dust  
 362 parametrisation was employed in the CTL and COVID simulations.

363

## 364 **Appendix B: Comparison of AOD over Western, Central, Eastern Himalayas and** 365 **Tibetan Plateau regions**

366 We elaborate on the comparison of MODIS AOD with our model simulations over  
 367 Western, Central, Eastern Himalayas and Tibetan Plateau regions (Fig. S5). Both MODIS and  
 368 the model show a reduction in AOD during spring 2020 over the aforementioned regions of  
 369 HKH. The estimated differences in AOD during March to May 2020 vary between 0.8 – 11%  
 370 over Western and Central Himalayas, and 8 – 16% over Eastern Himalayas. Over the Tibetan  
 371 plateau region, in contrast to the model simulations, MODIS shows an enhancement (2 – 16 %)  
 372 in AOD (Fig. S5). This may be due to dust aerosols, which are transported during spring from



373 western Asia and locally, generating dust piles over the Tibetan Plateau (ednavis et al., 2017,  
374 2021). The simulated dust aerosol concentration in spring 2020 over the Tibetan Plateau region  
375 is smaller than no COVID situation (Fig. S1c, Fig. S2). The simulated dust is a response to  
376 meteorology difference between the COVID and CTL simulations (Fig. S6).



377 References:

- 378 Bair, E., Stillinger, T., Rittger, K. & Skiles, M. COVID-19 lockdowns show reduced pollution  
 379 on snow and ice in the Indus River Basin. *Proc. Natl. Acad. Sci. U. S. A.* 118, 19–21,  
 380 <https://doi.org/10.1073/pnas.2101174118>, 2021.
- 381 Bolch, T. *et al.* Status and Change of the Cryosphere in the Extended Hindu Kush Himalaya  
 382 Region. in *The Hindu Kush Himalaya Assessment: Mountains, Climate Change,*  
 383 *Sustainability and People* (eds. Wester, P., Mishra, A., Mukherji, A. & Shrestha, A. B.)  
 384 209–255 (Springer International Publishing). doi:10.1007/978-3-319-92288-1\_7 2019,  
 385 2019.
- 386 Cruz, R.V., Harasawa, H., Lal, M., Wu, S, Anokhin, Y., Punsalmaa, B., Honda, Y., Jafari, M.,  
 387 Li, C., and Huu Ninh, N. Climate change 2001: impacts, adaptation, and vulnerability.  
 388 *Choice Rev. Online* 39, 39-3433-39-3433, 2007.
- 389 Fadnavis, S., Kalita, G., Ravi Kumar, K., Gasparini, B. & Li, J. L. F. Potential impact of  
 390 carbonaceous aerosol on the upper troposphere and lower stratosphere (UTLS) and  
 391 precipitation during Asian summer monsoon in a global model simulation. *Atmos. Chem.*  
 392 *Phys.* 17, 11637–11654, <https://doi.org/10.5194/acp-17-11637-2017>, 2017.
- 393 Fadnavis, S., Sabin T. P., Rap A., Müller R., Kubin A. and Heinold B., The impact of COVID-  
 394 19 lockdown measures on the Indian summer monsoon. *Environ. Res. Lett.* 16, DOI  
 395 10.1088/1748-9326/ac109c, 2021.
- 396 Fadnavis, S. Müller R., Chakraborty T., Sabin T. P., Laakso A., Rap A., Griessbach S., Vernier  
 397 J-P. & Tilmes S. The role of tropical volcanic eruptions in exacerbating Indian droughts.  
 398 *Sci. Rep.* 11, 1–13, <https://doi.org/10.1038/s41598-021-81566-0>, 2021.
- 399 Fadnavis, S. Müller R., Kalita G, Rowlinson M., Rap A., Frank Li J-L, Gasparini B, and  
 400 Laakso A. The impact of recent changes in Asian anthropogenic emissions of SO<sub>2</sub> on sulfate  
 401 loading in the upper troposphere and lower stratosphere and the associated radiative  
 402 changes.. *Atmos. Chem. Phys.* 1–44, <https://doi.org/10.5194/acp-19-9989-2019>, 2019a.
- 403 Fadnavis, S. Sabin T. P., Roy C., Rowlinson M, Rap A, Vernier J-P. & E. Sioris C. E.. Elevated  
 404 aerosol layer over South Asia worsens the Indian droughts. *Sci. Rep.* 9, 1–12,  
 405 <https://doi.org/10.1038/s41598-019-46704-9>, 2019b.
- 406 Forster, P. M. *et al.* Current and future global climate impacts resulting from COVID-19. *Nat.*



- 407 *Clim. Chang.* 10, 913–919, 2020.
- 408 Gogoi, M. M. S. Babu S., Arun B. S., Krishna, Moorthy K., Ajay A., Ajay P., Suryavanshi A.,  
 409 Borgohain A., *et al.* Response of Ambient BC Concentration Across the Indian Region to  
 410 the Nation-Wide Lockdown: Results from the ARFINET Measurements of ISRO-GBP.  
 411 *Curr. Sci.* 120, 341, doi: 10.18520/cs/v120/i2/341-351, 2021.
- 412 Hall, D. K. MODIS / Terra Snow Cover 5-Min L2 Swath 500m. *Color. USA NASA Natl. Snow*  
 413 *Ice Data Cent. Distrib. Act. Arch. Cent* 5, 2006.
- 414 Huang, W. T. K. Aerosol effects on climate, with an emphasis on the Arctic.  
 415 <https://doi.org/10.3929/ethz-b-000319114> 2018, 2018
- 416 Hussain, A. Sarangi G.K., Pandit A., Ishaq S., Mammun N., Ahmad B., Jamil M.K., Hydropower  
 417 development in the Hindu Kush Himalayan region: Issues, policies and opportunities.  
 418 *Renew. Sustain. Energy Rev.* 107, 446–461, <https://doi.org/10.1016/j.rser.2019.03.010>,  
 419 2019.
- 420 Hock, R. *et al.* Chapter 2: High Mountain Areas. IPCC Special Report on the Ocean and  
 421 Cryosphere in a Changing Climate. *IPCC Spec. Rep. Ocean Cryosph. a Chang. Clim.* 131–  
 422 202, 2019.
- 423 IPCC Working Group 1, I. *et al.* IPCC, 2013: Climate Change 2013: The Physical Science  
 424 Basis. Contribution of Working Group I to the Fifth Assessment Report of the  
 425 Intergovernmental Panel on Climate Change. *Ippc AR5*, 1535, 2013.
- 426 Lamarque J.-F. , Bond T. C., Eyring V., Granier C., Heil A., Klimont Z., Lee D., Liousse  
 427 C., Mieville A., Owen B., Schultz M. G., Shindell D., Smith S. J., Stehfest E., Aardenne  
 428 J. Van, Cooper O. R., Kainuma M., Mahowald N., McConnell J. R., Naik V., Riahi K.,  
 429 and Vuuren D. P. van, Historical (1850–2000) gridded anthropogenic and biomass burning  
 430 emissions of reactive gases and aerosols: Methodology and application. *Atmos. Chem.*  
 431 *Phys.* 10, 7017–7039, <https://doi.org/10.5194/acp-10-7017-2010>, 2010.
- 432 Kanniah, K. D., Kamarul Zaman, N. A. F., Kaskaoutis, D. G. & Latif, M. T. COVID-19’s  
 433 impact on the atmospheric environment in the Southeast Asia region. *Sci. Total Environ.*  
 434 736, 139658, <https://doi.org/10.1016/j.scitotenv.2020.1396580048-9697>, 2020.
- 435 Krishnan, R., Shrestha, A., Ren, G., Rajbhandari, R., Saeed, S., & Sanjay, J. Unravelling  
 436 Climate Change in the Hindu Kush Himalaya: Rapid Warming in the Mountains and  
 437 Increasing Extremes. *The Hindu Kush Himalaya Assessment* (Springer Singapore).



- 438      doi:10.1007/978-3-319-92288-1\_3, 2019.1
- 439      Krishnan, R. *et al.* Assessment of climate change over the Indian region: A report of the  
 440      ministry of earth sciences (MOES), government of India. Assessment of Climate Change  
 441      over the Indian Region: A Report of the Ministry of Earth Sciences (MoES), Government  
 442      of India (Springer Singapore). doi:10.1007/978-981-15-4327-2, 2020.
- 443      Lau, W. K. M., Kim, M. K., Kim, K. M. & Lee, W. S. Enhanced surface warming and  
 444      accelerated snow melt in the Himalayas and Tibetan Plateau induced by absorbing aerosols.  
 445      *Environ. Res. Lett.* 5, doi:10.1088/1748-9326/5/2/025204, 2010.
- 446      Lee, S. S., Chu, J. E., Timmermann, A., Chung, E. S. & Lee, J. Y. East Asian climate response  
 447      to COVID-19 lockdown measures in China. *Sci. Rep.* 11, 1–9, 2021a.
- 448      Lee, E., Carrivickl J. L., Quincey D. J., Cook S. J., Amesl W. H. M., & Brown L. E.,  
 449      Accelerated mass loss of Himalayan glaciers since the Little Ice Age. *Sci. Rep.* 11, 1–8,  
 450      <https://doi.org/10.1038/s41598-021-03805-8>, 2021b.
- 451      Le Quéré, C. Jackson R. B., Jones M. W., Smith A. J. P., Abernethy S. Andrew R. M., De-  
 452      Goll A. J. Willis D. R., Shan Y., Canadell J. G., Friedlingstein P., Creutzig F. and Peters G.  
 453      P., Temporary reduction in daily global CO<sub>2</sub> emissions during the COVID-19 forced  
 454      confinement. *Nat. Clim. Chang.* 10, 647–653, <https://doi.org/10.1038/s41558-020-0797-x>,  
 455      2020.
- 456      Liu, Y. Wang Y., Cao Y., Yang Xi, Zhang T., Luan M., Lyu D., Hansen A. D. A., Liu B., and  
 457      Zheng M., Impacts of COVID-19 on Black Carbon in Two Representative Regions in  
 458      China: Insights Based on Online Measurement in Beijing and Tibet. *Geophys. Res. Lett.*  
 459      48, 1–11, 10.1029/2021GL092770, 2021.
- 460      Ma, J. Zhang T., and GUAN X., The dominant role of snow/ice Albedo feedback strengthened  
 461      by black carbon in the enhanced warming over the Himalayas. *J. Clim.* 32, 5883–5899,  
 462      <https://doi.org/10.1175/JCLI-D-18-0720.s1>.2019.
- 463      Martonchik, J. V., Diner, D. J., Kahn, R., Gaitley, B. & Holben, B. N. Comparison of MISR  
 464      and AERONET aerosol optical depths over desert sites. *Geophys. Res. Lett.* 31, 1–  
 465      4, <https://doi.org/10.1029/2004GL019807>, 2004. \
- 466      Nair, V. S. Babu S. S., Moorthy K. K., Sharma A. K., Marinoni A. & Ajai, Black carbon aerosols  
 467      over the Himalayas: Direct and surface albedo forcing. *Tellus, Ser. B Chem. Phys.*



- 468 *Meteorol.* 65, DOI: 10.3402/tellusb.v65i0.19738, 2013.\
- 469 Pandey, S. K. & Vinoj, V. Surprising changes in aerosol loading over india amid covid-19  
 470 lockdown. *Aerosol Air Qual. Res.* 21, 1–12, <https://doi.org/10.4209/aaqr.2020.07.0466>,  
 471 2021.
- 472 Qian, Y., Flanner, M. G., Leung, L. R. & Wang, W. Sensitivity studies on the impacts of Tibetan  
 473 Plateau snowpack pollution on the Asian hydrological cycle and monsoon climate. *Atmos.*  
 474 *Chem. Phys.* 11, 1929–1948, doi:10.5194/acp-11-1929-2011, 2011. Sabin, T., Krishnan,  
 475 R., Vellore, R., Priya, P., Borgaonkar, H., Singh, B., Sagar, A. Droughts and floods.  
 476 Climate Change Over the Himalayas. Assessment Of Climate Change Over The Indian  
 477 Region. doi:10.1007/978-981-15-4327-2\_11, 2020.
- 478 Rogelj, J. Schaefferc M., Meinshausene M., Shindell D. T, Harec W., Klimontb Z. , Veldersh  
 479 G. J. M., Amannb M., and Schellnhuberr H.J., Disentangling the effects of CO2 and short-  
 480 lived climate forcer mitigation. *Proc. Natl. Acad. Sci. U. S. A.* 111, 16325–16330,  
 481 <https://doi.org/10.1073/pnas.1415631111>, 2014.
- 482 Santra, S. Verma1 S., Fujita K, Chakraborty I, Boucher O., Takemura T., Burkhardt John F.,  
 483 Matt F, and Sharma M., Simulations of black carbon (BC) aerosol impact over Hindu Kush  
 484 Himalayan sites: Validation, sources, and implications on glacier runoff. *Atmos. Chem.*  
 485 *Phys.* 19, 2441–2460, <https://doi.org/10.5194/acp-19-2441-2019>, 2019.
- 486 Sarangi, C. Qian Y., Rittger K., Bormann K.J., Liu Y., Wang H., Wan H., Lin G., and. Painter  
 487 T.H., Impact of light-absorbing particles on snow albedo darkening and associated  
 488 radiative forcing over high-mountain Asia: high-resolution WRF-Chem modeling and new  
 489 satellite observations. *Atmos. Chem. Phys.* 19, 7105–7128, [https://doi.org/10.5194/acp-19-](https://doi.org/10.5194/acp-19-7105-2019)  
 490 7105-2019, 2019.
- 491 Schultz, M. G., Stadtler S., Schröder S., Taraborrelli D., Franco B., Krefting J, Henrot A. et  
 492 al., The chemistry-climate model ECHAM6.3-HAM2.3-MOZ1.0. *Geosci. Model Dev.* 11,  
 493 1695–1723, <https://doi.org/10.5194/gmd-11-1695-2018>, 2018.
- 494 Shafeeque, M. Arshad A., A Elbeltagi A., Sarwar A., Pham Q. B., S Khan S. N., l Dilawar A.  
 495 & Al-Ansari N., Understanding temporary reduction in atmospheric pollution and its  
 496 impacts on coastal aquatic system during COVID-19 lockdown: a case study of South Asia.  
 497 *Geomatics, Nat. Hazards Risk* 12, 560–580,  
 498 <https://doi.org/10.1080/19475705.2021.1885503>, 2021.





- 499 Srivastava, A. K., Bhoyar P.D., Kanawade V. P., Devara P.C. S., Thomas A., Soni V.K.,  
 500 Improved air quality during COVID-19 at an urban megacity over the Indo-Gangetic Basin:  
 501 From stringent to relaxed lockdown phases. *Urban Clim.* 36, 100791,  
 502 <https://doi.org/10.1016/j.uclim.2021.100791>, 2021.
- 503 Stevens, B., Giorgetta M., Esch M., Mauritsen T., Crueger T., Rast S., Salzmann M., Schmidt  
 504 H., Bader J., Block K., Brokopf R., Fast I., Kinne S., Kornblueh L., Lohmann U., Pincus  
 505 R., Reichler T., Roeckner E. Atmospheric component of the MPI-M earth system model:  
 506 ECHAM6. *J. Adv. Model. Earth Syst.* 5, 146–172, <https://doi.org/10.1002/jame.20015>,  
 507 2013.
- 508 Stier, P., Feichter J., Kinne S., Kloster S., Vignati E., Wilson J., Ganzeveld L., Tegen  
 509 I., Werner M., Balkanski Y., Schulz M., Boucher O., Minikin A., and Petzold A., The  
 510 aerosol-climate model ECHAM5-HAM. *Atmos. Chem. Phys.* 5, 1125–1156,  
 511 <https://doi.org/10.5194/acp-5-1125-2005>, 2005.
- 512 Tegen, I., Neubauer D., Ferrachat S., Siegenthaler-Le Drian C, Bey, I., Schutgens N., Stier P.,  
 513 Watson-Parris D., et al., The global aerosol-climate model echam6.3-ham2.3 -Part 1:  
 514 Aerosol evaluation. *Geosci. Model Dev.* 12, 1643–1677, [https://doi.org/10.5194/gmd-12-](https://doi.org/10.5194/gmd-12-1643-2019)  
 515 1643-2019, 2019.
- 516 Thind, P. S., Chandel, K. K., Sharma, S. K., Mandal, T. K. & John, S. Light-absorbing  
 517 impurities in snow of the Indian Western Himalayas: impact on snow albedo, radiative  
 518 forcing, and enhanced melting. *Environ. Sci. Pollut. Res.* 26, 7566–7578,  
 519 <https://doi.org/10.1007/s11356-019-04183-5>, 2019.
- 520 Textor, Schulz M., Guibert S., Kinne S., Balkanski Y., Bauer S., Bernsten T., Berglen  
 521 T., Boucher O., Chin M., Dentener F., Diehl<sup>1</sup> T., Easter R., Feichter H., Fillmore  
 522 D., Ghan S., Ginoux P., Gong S., Grini A., Hendricks J., Horowitz L., Huang  
 523 P., Isaksen I., Iversen I., Kloster S., Koch D., Kirkevåg A., Kristjansson J. E., Krol M.  
 524 , Lauer A., Lamarque J. F., Liu X., Montanaro V., Myhre G., Penner J., Pitari  
 525 G., Reddy<sup>5</sup> S., Seland Ø., Stier P., Takemura T., and Tie X., Analysis and quantification  
 526 of the diversities of aerosol life cycles within AeroCom. *Atmos. Chem. Phys.* 6, 1777–1813,  
 527 <https://doi.org/10.5194/acp-6-1777-2006>, 2006.
- 528 Tiwari, S., Kar, S. C. & Bhatla, R. Snowfall and Snowmelt Variability over Himalayan Region  
 529 in Inter-annual Timescale. *Aquat. Procedia* 4, 942–949, doi: 10.1016/j.aqpro.2015.02.118,



- 530 2015.
- 531 Usha, K. H., Nair, V. S. & Babu, S. S. Effect of aerosol-induced snow darkening on the direct  
 532 radiative effect of aerosols over the Himalayan region. *Environ. Res. Lett.* 16,  
 533 <https://doi.org/10.1088/1748-9326/abf190>, 2021.
- 534 Wester P., Mishra A., Mukherji A., S. A. B. The Hindu Kush Himalaya Assessment—  
 535 Mountains, Climate Change, Sustainability and People. Springer Nature Switzerland AG,  
 536 Cham. doi:<https://doi.org/10.1007/978-3-319-92288-1>, 2019.
- 537 Wood, L. R. Neumann K., Nicholson K.N., Bird B.W., Dowling C. B. and Sharma S. Melting  
 538 Himalayan Glaciers Threaten Domestic Water Resources in the Mount Everest Region,  
 539 Nepal. *Front. Earth Sci.* 8, 1–8, <https://doi.org/10.3389/feart.2020.00128>, 2020.
- 540 Zhang, K. O'Donnell D., Kazil J., Stier P., Kinne S., Lohmann U., Ferrachat S., Croft B.,  
 541 Quaas J, Wan H., Rast S., and Feichter J., The global aerosol-climate model ECHAM-  
 542 HAM, version 2: Sensitivity to improvements in process representations. *Atmos. Chem.*  
 543 *Phys.* 12, 8911–8949, <https://doi.org/10.5194/acp-12-8911-2012>, 2012.

544

## 545 Acknowledgments



546 The authors thank the staff of the High Power Computing Centre (HPC) in IITM, Pune, India,  
 547 for providing computer resources and the team members of MODIS for providing data. We  
 548 thank Sabur F. Abdullaev and Brent Holben for their efforts in establishing and maintaining  
 549 Dushanbe and Lahore AERONET sites respectively.

## 550 Author Contributions

551 S.F. initiated the idea of the study. S.F., B. H. and K. H. designed and performed model  
 552 simulations. K. H. included a 'BC in snow' scheme in the ECHAM6-HAMMOZ model. A.R.  
 553 and A. K. prepared Google based emission inventory. T.P.S., R.M. performed data analysis  
 554 and contributed in overall design. All authors contributed to discussions of the results and the  
 555 writing of the manuscript.



556 **Data and code availability**

557 The ECHAM-HAMMOZ model source code and all required input data are available to the  
558 scientific community according to the HAMMOZ Software License Agreement through the  
559 project website: <https://redmine.hammoz.ethz.ch/projects/hammoz>. The data that support the  
560 findings of this study are openly available in zenodo at DOI 10.5281/zenodo.6783077

561

562 **Competing Interests:** The authors declare no competing interests.

563

564